Inorg. Chem. **2002**, *41*, 2496–2504

Structure and Bonding in the Aluminum Radical Species Al·NH_3, $HAlNH_2$, $HAlNH_2$·NH_3, and $Al(NH_2)_2$ Studied by Means of Matrix IR Spectroscopy and Quantum Chemical Calculations

Benjamin Gaertner and Hans-Jörg Himmel*

Institut für Anorganische Chemie, Universität Karlsruhe (TH), Engesserstrasse Geb. 30.45, 76128 Karlsruhe, Germany

Received December 18, 2001

Experimental matrix IR spectra in alliance with extensive quantum chemical calculations provide a framework for the detailed evaluation of the structures and electronic properties of the doublet species Al·NH_3, $Al(NH_3)_2$, $HAlNH_2$, $HAlNH_2$·NH_3, and $Al(NH_2)_2$. These species were the products of the reaction of Al atoms with NH_3 in an Ar matrix. While the two species Al·NH_3 and $HAlNH_2$ were already sighted in previous experiments, the results described herein lead to the first identification and characterization of $HAlNH_2$·NH_3 and $Al(NH_2)_2$, the products of the reaction of Al atoms with two NH_3 molecules. The results allow a detailed reaction scheme leading to all the product species to be established. The unpaired electron in each of the species Al·NH_3, $Al(NH_3)_2$, $HAlNH_2$, $HAlNH_2$·NH_3, and $Al(NH_2)_2$ is located near the Al atom, but there is a significant degree of delocalization, especially in $Al(NH_2)_2$, due to π bonding interactions. The consequences for the barrier to pyramidalization at the N-atom are discussed.

Introduction

There is an ongoing interest in low valent compounds of group 13 elements, despite or, more likely, even stimulated by the fact that they are commonly highly unstable toward disproportionation.[1] Thus, aluminum usually does not occur as Al(II), and only under special conditions, for example, in an inert gas matrix at temperatures as low as 10−30 K, can these species be generated and characterized at leisure. Otherwise, they can be isolated only in the form of their dimers or oligomers, often featuring Al−Al bonds and therefore exhibiting not a doublet, but a singlet electronic ground state, for example, $[Al\{CH(SiMe_3)_2\}_2]_2$[2] and Al_2I_4·$2Et_2O$.[3] Not much more is known about Al(I) species. Again, oligomerization prevents the isolation of monomers in most cases, for example, $[Et_3N{\cdot}AlBr]_4$[4] or $Al_4(C_5Me_5)_4$.[5] There are also known some cluster compounds, for example, $[Al_{77}\{N(SiMe_3)_2\}_{20}]$[6] or $[Al_{69}\{N(SiMe_3)_2\}_{18}]$,[7] featuring low valent Al atoms (the latter showing interesting paramagnetic behavior). Knowledge of what are formally Al(0) species with a doublet electronic ground state again is restricted to a very few systems, and we owe nearly all of the sparse information we have about these species to matrix isolation or gas-phase experiments. In the past, the Al(II) hydrides HAlH,[8] CH_3AlH,[9] $HAlNH_2$,[10,11] $HAlPH_2$,[12,13] and HAlOH[14] have been identified and characterized in solid inert gas matrixes, mostly on the basis of their IR spectra, but, in the case of HAlH,[15] also by EPR. Simple Al(I) species which were studied in similar experiments include the halides AlX (X = F, Cl, Br), $AlNH_2$,[10,11] AlH,[16] and AlOH,[14] but also

* To whom correspondence should be addressed. E-mail: himmel@achpc9.chemie.uni-karlsruhe.de.

(1) Downs, A. J. *Coord. Chem. Rev.* **1999**, *189*, 59. Downs, A. J.; Himmel, H.-J.; Manceron, L. *Polyhedron*, in press.
(2) Uhl, W. *Angew. Chem., Int. Ed. Engl.* **1993**, *32*, 1386.
(3) Ecker, A.; Baum, E.; Friesen, M. A.; Junker, M. A.; Üffing, C.; Köppe, R.; Schnöckel, H. *Z. Anorg. Allg. Chem.* **1998**, *3*, 513.
(4) Mocker, M.; Robl, C.; Schnöckel, H. *Angew. Chem.* **1994**, *106*, 1860; *Angew. Chem., Int. Ed. Engl.* **1994**, *33*, 1754.
(5) Dohmeier, C.; Robl, C.; Tacke, M.; Schnöckel, H. *Angew. Chem.* **1991**, *103*, 594; *Angew. Chem., Int. Ed. Engl.* **1991**, *30*, 564.
(6) Ecker, A.; Weckert, E.; Schnöckel, H. *Nature* **1997**, *387*, 379.
(7) Köhnlein, H.; Purath, A.; Klemp, C.; Baum, E.; Krossing, I.; Stösser, G.; Schnöckel, H. *Inorg. Chem.* **2001**, *40*, 4830.
(8) Parnis, J. M.; Ozin, G. A. *J. Phys. Chem.* **1989**, *93*, 1215. Chertihin, G. V.; Andrews, L. *J. Phys. Chem.* **1993**, *97*, 10295. Pullumbi, P.; Mijoule, C.; Manceron, L.; Bouteiller, Y. *Chem. Phys.* **1994**, *185*, 13.
(9) Parnis, J. M.; Ozin, G. A. *J. Phys. Chem.* **1989**, *93*, 1204, 1220.
(10) Lanzisera, D. V.; Andrews, L. *J. Phys. Chem. A* **1997**, *101*, 5082.
(11) Himmel, H.-J.; Downs, A. J.; Greene, T. M. *J. Am. Chem. Soc.* **2000**, *122*, 9793.
(12) Himmel, H.-J.; Downs, A. J.; Greene, T. M. *Inorg. Chem.* **2001**, *40*, 396.
(13) Himmel, H.-J.; Downs, A. J.; Green, J. C.; Greene, T. M. *J. Chem. Soc., Dalton Trans.* **2001**, 535.
(14) Hauge, R. H.; Kauffman, J. W.; Margrave, J. L. *J. Am. Chem. Soc.* **1980**, *102*, 6005.

10.1021/ic011292n CCC: $22.00
Published on Web 04/09/2002

the doubly bridged species $Al(\mu\text{-}H)_2Al$.[17] Finally, Al·CO,[18] Al·SiH_4,[19,20] Al·NH_3,[11] Al·N_2,[21] and Al·PH_3[12] are adducts of the bare atoms that have been identified with varying degrees of confidence in inert gas matrixes. The preliminary experiments point to interesting and unusual electronic, as well as structural, properties of these species. In addition to this fundamental aspect, the interest in weak complexes in general is spurred by the fact that they act as the first intermediates in many reactions and therefore hold a vital key to the knowledge of reaction mechanisms which is essential to control reactivity and product distributions. Last but not least, molecules such as the ones addressed in this work, featuring a bond between a group 13 and a group 15 element, represent potential intermediates or model compounds for chemical vapor deposition (CVD) processes leading to semiconductor materials.[22]

Herein, we give a detailed account of the matrix reactions of Al atoms with one and two NH_3 molecules studied experimentally by IR spectroscopy and theoretically by applying ab initio and DFT methods. Al·NH_3, $Al(NH_3)_2$, $AlNH_2$, $HAlNH_2$, $HAlNH_2$·NH_3, $Al(NH_2)_2$, and H_2AlNH_2 are the identifiable products, and five of these [Al·NH_3, $Al(NH_2)_2$, $HAlNH_2$, $HAlNH_2$·NH_3, and $Al(NH_2)_2$] should exhibit doublet electronic states. These five species are the focus of the present work. While experimental data for the reaction of Al atoms with one NH_3 molecule are already available, this is the first account of the reaction with two NH_3 molecules. Moreover, the photolysis sequences for the reaction with one NH_3 molecule have been modified, with consequences for the reaction mechanisms.

Experimental Section

Al atoms were emitted from a Knudsen cell type evaporator, which was resistively heated to 1100 °C, and co-deposited together with NH_3 in an excess of argon on a freshly polished copper block which was cooled to 12 K by a closed-cycle refrigerator from Leybold. Details of the apparatus and other experimental techniques can be found elsewhere.[23]

IR spectra were taken with the aid of a Bruker 113v spectrometer equipped with a liquid N_2 cooled MCT and a DTGS detector for measurements in the range 4000−300 cm^{-1}.

The following chemicals with purities and sources quoted in parentheses were used: Al (99.99%, Merck), NH_3 (>99.98%, Messer), ND_3 (99-atom %, Aldrich), $^{15}NH_3$ (98-atom %, Aldrich), and Ar (99.998%, Messer).

Quantum chemical calculations relied on the TURBOMOLE[24] program package applying ab initio (MP2) and DFT (BP) methods together with a TZVPP basis set. In the following, the values calculated with the MP2 and BP methods are quoted in the order MP2/BP.

Results

Figure 1, spectrum i displays the IR spectrum taken upon co-deposition of Al atoms together with 5% NH_3 in an Ar matrix. The spectrum contains strong absorptions characteristic of NH_3 and very weak ones due to traces of impurities (H_2O, CO_2, CO, HAlOH),[25] and in addition two absorptions at 1132.0 and 1593.6 cm^{-1} belonging to a first product **A** of the reaction of Al atoms with NH_3. These absorptions were previously associated with the adduct Al·NH_3.[11] There followed a period of photolysis with light having $\lambda = \sim 580$ nm to give the corresponding IR spectrum displayed in Figure 1, spectrum ii. This treatment resulted in the extinction of the signals due to **A** and the massive growth of two sets of absorptions belonging to two distinct products **C** and **D**. Product **C**, with as many as eight bands, appeared at 3476.4, 1761.1, 1533.6, 778.6, 704.8, 483.8, 482.2, and 393.8 cm^{-1}. These signals were already observed in previous studies[10,11] and assigned to the insertion product $HAlNH_2$. Note that this species was previously generated by photolysis of the matrix not with $\lambda = \sim 580$ nm light, but with $\lambda = \sim 440$ nm light, corresponding to the absorption maximum of Al·NH_3. Product **D** is characterized by three bands at 1739.3, 1196.2, and 734.7 cm^{-1}. These were not observed in the previous experiments, most likely because of the different photolysis conditions applied therein. Subsequently, the matrix was subjected to a period of photolysis at $\lambda = \sim 370$ nm [see Figure 1, spectrum iii]. The signals due to product **C** were only slightly affected, whereas the signals due to product **D** decreased almost to vanishing point. At the same time, four new absorptions due to product **E** were observed to grow in. These were located at 3485.3, 1525.1, 833.6, and 748.2 cm^{-1}. Upon photolysis at wavelengths near 420 nm, the signals due to **C** were extinguished, while those due to **E** were not affected. Following further photolysis with broadband UV−vis radiation ($200 < \lambda < 800$ nm), the signals due to **E** were also found to decay. Simultaneously with the disappearance of the signals due to **C** and **E**, two sets of signals appeared with wavenumbers of 3495.1, 1520.1, 726.5, 406.5 cm^{-1} and 3499.7, 1899.3, 1891.0, 1541.6, 818.7, 769.8, 755.0, 608.7, 518.3 cm^{-1}. These were already reported in previous studies[10,11] and associated with the products $AlNH_2$ and H_2AlNH_2.

In experiments in which $^{14}NH_3$ was replaced by $^{15}NH_3$, all signals due to species **A**, **C**, **D**, and **E** experienced red shifts. One of the signals due to species **A** now occurred at 1125.6 cm^{-1}, and those of **C**, at 3468.2, 1761.0, 1531.5,

(15) Knight, L., Jr.; Woodward, J. R.; Kink, T.; Arrington, C. A. *J. Phys. Chem.* **1993**, *97*, 1304.
(16) Pullumbi, P.; Mijoule, C.; Manceron, L.; Bouteiller, Y. *Chem. Phys.* **1994**, *185*, 13.
(17) Stephens, J. C.; Bolton, E. E.; Schaefer, H. F., III.; Andrews, L. *J. Chem. Phys.* **1997**, *107*, 119.
(18) Xu, C.; Manceron, L.; Perchard, J. P. *J. Chem. Soc., Faraday Trans.* **1993**, *89*, 1291.
(19) Lefcourt, M. A.; Ozin, G. A. *J. Phys. Chem.* **1991**, *95*, 2616.
(20) Gaertner, B.; Himmel, H.-J. *Angew. Chem.*, in press.
(21) Himmel, H.-J.; Downs, A. J. Unpublished results.
(22) *Chemistry of Aluminium, Gallium, Indium and Thallium*; Downs, A. J., Ed.; Blackie: Glasgow, U.K., 1993.
(23) See, for example: Himmel, H. J.; Downs, A. J.; Greene, T. M.; Andrews, L. *Organometallics* **2000**, *19*, 1060. Zumbusch, A.; Schnöckel, H. *J. Chem. Phys.* **1998**, *108*, 8092.
(24) Ahlrichs, R.; Bär, M.; Häser, M.; Horn, H.; Kölmel, C. *Chem. Phys. Lett.* **1989**, *162*, 165. Eichkorn, K.; Treutler, O.; Öhm, H.; Häser, M.; Ahlrichs, R. *Chem. Phys. Lett.* **1995**, *240*, 283. Eichkorn, K.; Treutler, O.; Öhm, H.; Häser, M.; Ahlrichs, R. *Chem. Phys. Lett.* **1995**, *242*, 652. Eichkorn, K.; Weigend, F.;. Treutler, O.; Ahlrichs, R. *Theor. Chem. Acc.* **1997**, *97*, 119. Weigend, F.; Häser, M. *Theor. Chem. Acc.* **1997**, *97*, 331. Weigend, F.; M. Häser, M.; Patzelt, H.; Ahlrichs, R. *Chem. Phys. Lett.* **1998**, *294*, 143.
(25) Greene, T. M.; Andrews, L.; Downs, A. J. *J. Am. Chem. Soc.* **1995**, *117*, 8180.

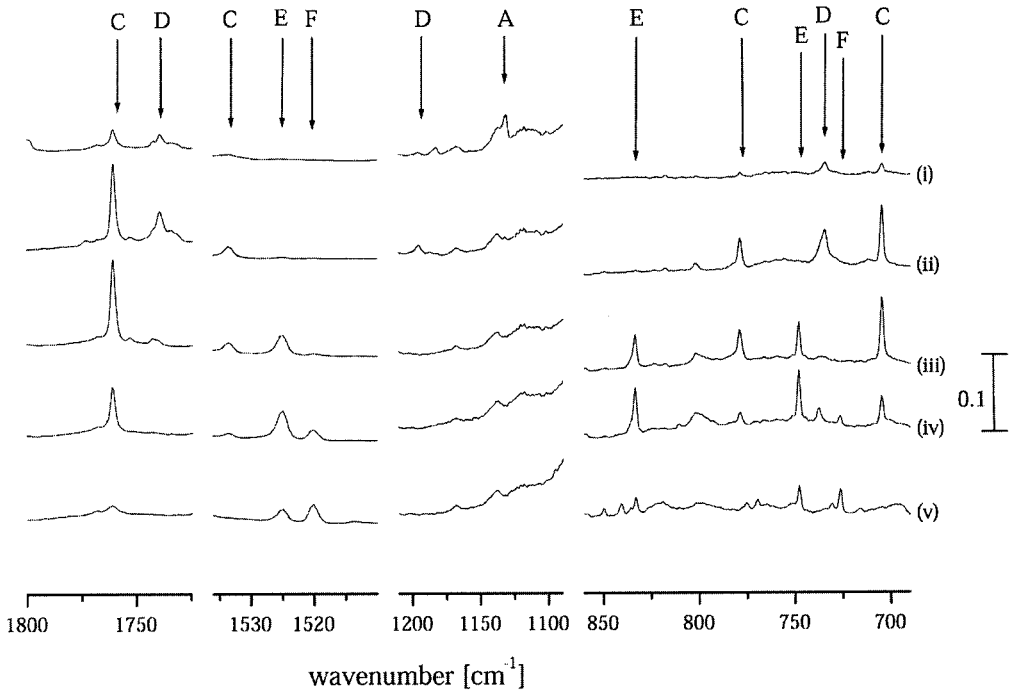

Figure 1. IR spectra obtained for the reaction of Al atoms with NH_3 in an Ar matrix: (i) following deposition; (ii) following photolysis at $\lambda = \sim 580$ nm; (iii) following photolysis at $\lambda = \sim 370$ nm; (iv) following photolysis at $\lambda = \sim 420$ nm; and (v) following broad-band UV−vis photolysis ($\lambda = 200-800$ nm).

766.9, 701.0, 483.2, 391.9 cm^{-1}. The signals due to species **D** were shifted to 1738.9 and 730.7 cm^{-1}, and those of species **E** appeared at 1520.0, 821.4, and 742.9 cm^{-1}.

Additional experiments were performed with ND_3 in place of NH_3. The signals due to species **A** and **C** appeared at 972.6 cm^{-1} and 2595.6, 1282.6, 1151.4, 748.3, 549.8, 346.5, 314.6, 304.6 cm^{-1}, respectively. Signals due to species **D** in its deuterated version were not sighted either because of lack of intensity or because they were hidden by stronger ND_3 absorption. The signals due to **E** occurred at 1151.3 and 687.5 cm^{-1}.

Finally, an experiment was carried out with as much as 10% NH_3. In this experiment, all signals that appeared in the experiments with 5% NH_3 were detected, and the conditions of their appearance and decay were similar. However, the relative abundance of species **A**, **C**, **D**, and **E** altered. Thus, the signals assigned to products **D** and **E** gained intensity relative to those due to **A** and **C** for higher concentration of NH_3 in the matrix. For example, the signals due to species **D**, formed at the same stage as species **C**, doubled their intensities, while the signals assigned to product **C** decreased to almost a third of the intensities they had in the experiments with 5% NH_3. At the same time, all signals broadened somewhat, especially those due to product **D**. The obvious inference is that **A** and **C** are the products of the reaction with more than one NH_3 moiety.

Discussion

We will show in the following how the experimental results, together with quantum chemical calculations, enable us not only to identify the reaction products Al·NH_3 (**A**), $Al(NH_3)_2$ (**B**), $HAlNH_2$ (**C**), $HAlNH_2$·NH_3 (**D**), and $Al(NH_2)_2$ (**E**), all exhibiting doublet electronic ground states, but also to evaluate in detail their structures, bonding properties, and reactivities.

Al·NH_3 and $Al(NH_3)_2$, A and B. Species **A** was already identified previously as the adduct Al·NH_3,[11] but the conditions of its formation were different (see the Reaction Mechanisms section). The $\delta_{sym}(NH_3)$ mode of Al·NH_3 is *blue* shifted with respect to the corresponding mode of isolated NH_3. In a previous report, it was also mentioned that this blue shift is a first indication of an electron donation of the NH_3 group.[26] The effect parallels that observed for complexes of alkali metal atoms with NH_3. Our ab initio and DFT calculations agree with previous calculations[11,27] in predicting a Jahn−Teller distortion resulting in C_s rather than C_{3v} symmetry of the molecule, with one of the N−H bonds being slightly elongated. The exact dimensions as derived from both ab initio and DFT calculations are given in Table 1; the calculated wavenumbers are quoted in Table 2. Noteworthy is the short Al−N distance of 231.3−232.1 pm.

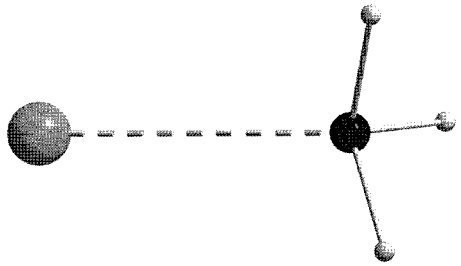

A, Al·NH_3

Figure 2 shows the MO scheme and the shapes of the frontier orbitals of the molecule. Both SOMO and LUMO

(26) Süzer, S.; Andrews, L. *J. Am. Chem. Soc.* **1987**, *109*, 300.
(27) Sakai, S. *J. Phys. Chem.* **1992**, *96*, 8369. Davy, R. D.; Jaffrey, K. L. *J. Phys. Chem.* **1994**, *98*, 8930.

Table 1. Calculated Dimensions of the Five Species Al·NH_3, Al$(NH_3)_2$, HAlNH_2·NH_3, HAlNH_2, Al$(NH_2)_2$; Distances in pm, Angles in deg

	Al·NH_3		Al$(NH_3)_2$		HAlNH_2·NH_3		HAlNH_2		Al$(NH_2)_2$	
parameter	MP2	BP	MP2	BP	MP2	BP	MP2	BP	MP2	BP
d(**Al**−**N**H_3) *d*(1−2)	231.3	232.1	231.4	235.1	209.2	211.6				
d(**N**−**H**$_3$) *d*(2−3)	101.4	102.3	101.3	102.3	101.3	102.3				
d(**N**−**H**$_3$) *d*(2−4)	101.4	102.3	101.3	102.3	101.3	102.4				
d(**N**−**H**$_3$) *d*(2−5)	101.3	102.3	101.4	102.2	101.5	102.6				
d(**Al**−**H**) *d*(1−6)					160.5	162.3	159.3	161.6		
d(**Al**−**N**H_2) *d*(1−7)					183.1	184.3	178.6	179.5	178.7	179.8
d(**N**−**H**$_2$) *d*(7−8)					100.8	101.8	100.6	101.5	101.7	101.5
d(**N**−**H**$_2$) *d*(7−9)					100.9	102.0	100.8	101.8	101.9	101.7
α(**Al**−**N**−**H**$_3$) α(1−2−3)	110.0	109.3	116.1	111.3	112.2	111.6				
α(**Al**−**N**−**H**$_3$) α(1−2−4)	110.0	109.3	116.2	120.2	114.5	114.0				
α(**Al**−**N**−**H**$_3$) α(1−2−5)	114.5	115.6	102.0	102.4	106.6	107.7				
α(**H**$_3$−**N**−**H**$_3$) α(3−2−4)	106.5	106.5	108.3	108.1	107.9	107.7				
α(**H**$_3$−**N**−**H**$_3$) α(3−2−5)	107.8	107.9	106.6	107.3	107.1	107.1				
α(**H**$_3$−**N**−**H**$_3$) α(4−2−5)	107.8	107.9	106.6	106.7	108.3	108.5				
α(NH_3−**Al**−NH_3) α(7−1−11)			83.3	87.8						
α(NH_3−**Al**−**N**H_2) α(7−1−2)					98.2	98.1				
α(**H**−**Al**−NH_3) α(2−1−6)					97.0	97.9				
α(**H**−**Al**−NH_2) α(6−1−7)					114.0	113.0	116.0	115.4		
α(**Al**−**N**−**H**$_2$) α(1−7−8)					112.1	118.7	125.5	125.5	124.0	123.8
α(**Al**−**N**−**H**$_2$) α(1−7−9)					120.1	121.3	124.6	124.6	125.6	126.2
α(**N**H_2−**Al**−**N**H_2) α(7−1−10)									119.7	119.4

Table 2. Calculated Wavenumbers (in cm^{-1}) for Al·$^{14}NH_3$, Al·$^{15}NH_3$, Al·$^{14}ND_3$, Al$(^{14}NH_3)_2$, Al$(^{15}NH_3)_2$, and Al$(^{14}ND_3)_2$ with IR Intensities (in km mol^{-1}) in Parentheses

Al·$^{14}NH_3$	Al·$^{15}NH_3$	Al·$^{14}ND_3$	assignment	Al$(^{14}NH_3)_2$	Al$(^{15}NH_3)_2$	Al$(^{14}ND_3)_2$	assignment
3490.5 (50)	3480.9 (50)	2568.9 (14)	a′	496.6 (34)	494.6 (34)	374.1 (18)	a
3369.3 (0.7)	3367.1 (1)	2406.3 (2)	a′	406.4 (1)	405.2 (1)	299.3 (1)	a
1610.1 (18)	1607.2 (18)	1166.9 (16)	a′	3500.0 (5)	3490.6 (5)	2575.9 (0.1)	a
1137.0 (115)	1131.1 (112)	864.6 (83)	a′	3497.6 (1)	3487.9 (1)	2575.5 (5)	a
458.6 (9)	457.1 (9)	340.2 (4)	a′	3371.1 (8)	3369.0 (8)	2407.3 (2)	a
241.5 (24)	237.4 (23)	229.8 (20)	a′	220.8 (8)	218.3 (7)	204.5 (8)	a
3491.3 (26)	3481.9 (26)	2571.6 (25)	a″	197.1 (2)	196.4 (2)	142.0 (0.1)	a
1608.0 (38)	1604.9 (38)	1166.4 (7)	a″	1616.0 (4)	1613.1 (4)	1171.0 (3)	a
446.5 (1)	445.4 (1)	327.6 (0.1)	a″	1597.7 (19)	1594.7 (18)	1158.9 (10)	a
				125.9 (8)	123.0 (8)	113.2 (7)	a
				1119.9 (64)	1114.3 (62)	849.5 (48)	a
				3499.5 (47)	3490.0 (46)	2575.5 (31)	b
				3495.7 (75)	3486.0 (76)	2574.2 (27)	b
				3371.3 (1)	3369.2 (1)	2407.4 (1)	b
				1610.6 (21)	1607.5 (22)	1168.7 (7)	b
				1594.0 (44)	1591.1 (44)	1155.0 (18)	b
				1107.0 (176)	1101.3 (173)	841.8 (116)	b
				417.3 (1)	416.2 (1)	307.5 (1)	b
				383.0 (1)	381.7 (1)	293.2 (0.4)	b
				200.1 (8)	198.3 (6)	178.2 (8)	b
				189.5 (4)	188.3 (5)	134.0 (3)	b

exhibit a pronounced Al 2p character. In Figure 3, the electron density distribution in the adduct is plotted. The polarization of the electron density in the direction from NH_3 toward Al is clearly visible. We also calculated the Mulliken charges (see Table 3) and obtained, in agreement with earlier studies,[28,29] a formal negative charge of −0.25 e on the Al atom. However, it has been argued that the Mulliken population analysis often gives misleading results.

In the following account, it will be shown that Al atoms are capable of binding not only one but two NH_3 moieties, giving rise to the species HAlNH_2·NH_3 and Al$(NH_2)_2$. The obvious precursor to these species is the bis adduct Al$(NH_3)_2$. The failure to detect any signal due to this species is likely to be caused by lack of IR intensity or signal broadening. Nevertheless, its structure and IR absorptions were calculated, all data being summarized in Tables 1 and 2. The ground-state symmetry is C_{2v}. The Al−N distance (209.2−211.6 pm) differs only slightly from the one found in Al·NH_3. The Mulliken formal charge calculated for the Al atom is at −0.43 e, not quite twice the value calculated for Al·NH_3. It is clear that this value is only a formal charge and cannot be taken too seriously. However, it indicates a clear trend toward partial negative charges for the adducts, underlining the electron-donor capacity of NH_3.

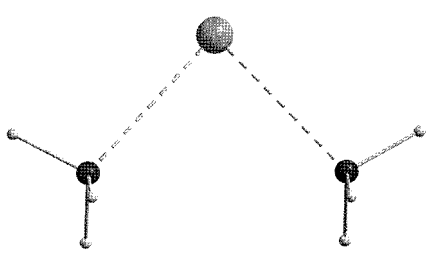

B, Al$(NH_3)_2$

(28) Davy, R. D.; Jaffrey, K. L. *J. Phys. Chem.* **1994**, *98*, 8930.
(29) Imura, K.; Kawashima, T.; Ohoyama, H.; Kasai, T. *J. Am. Chem. Soc.* **2001**, *123*, 6367.

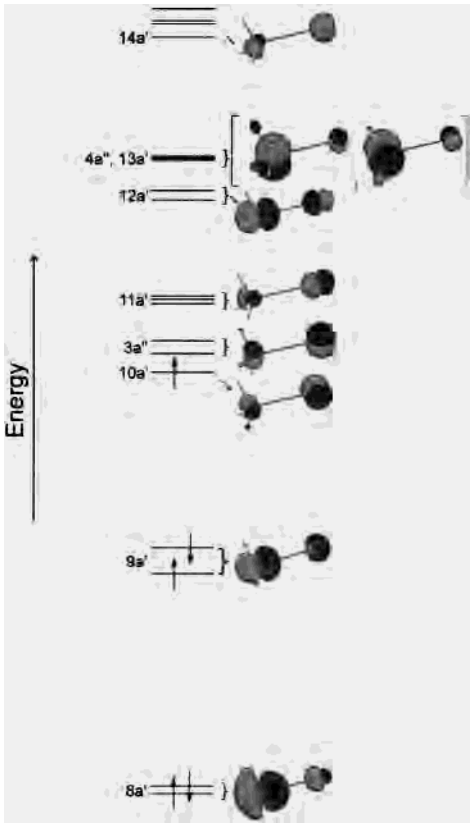

Figure 2. Plot showing the MO scheme and the shapes of the frontier orbitals for Al·NH_3.

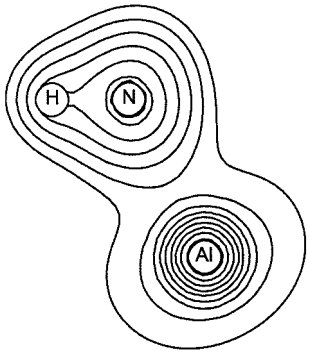

Figure 3. Plot showing the electron density distribution in Al·NH_3. Contour values (in 10^{-33} e m^{-3}): 2.96, 5.93, 11.9, 23.7, 47.4, 94.8, 190, 379, 759.

Table 3. Mulliken Charges (in e) for NH_3, Al·NH_3, and $Al(NH_3)_2$

	NH_3	Al·NH_3	$Al(NH_3)_2$
Al		−0.2531	−0.4320
N	−0.4647	−0.2482	−0.2712
H	0.1549	0.1747	0.1729
H	0.1549	0.1633	0.1672
H	0.1549	0.1633	0.1471

$HAlNH_2$ and $HAlNH_2$·NH_3, C and D. Like species **A**, **C** has been previously sighted in matrix experiments and identified as the radical species $HAlNH_2$. Our experiments hit on as many as 8 of the 9 vibrational fundamentals of the molecule. The π interaction between the Al and N p orbitals stabilizes the planar structure of the molecule.

Product **D** shows absorptions in the same region as those of $HAlNH_2$. Like $HAlNH_2$, it is formed upon photolysis of the matrix with light having $\lambda = \sim 580$ nm. As already mentioned, high concentrations of NH_3 favor the generation of **D** relative to **C** in the matrix. The obvious inference is that product **D** is the product of the reaction of Al atoms with two molecules of NH_3. Thus, the obvious candidate for this species is $HAlNH_2$·NH_3. This molecule was not sighted in any of the previous studies because of its immediate decomposition under the photolysis conditions chosen in those studies. Indeed, it shows a photochemistry distinctly different from that of $HAlNH_2$. While the latter is stable to photolysis at $\lambda = \sim 370$ nm, the former is converted into species **E** (see later). Our quantum chemical calculations resulted in a ground state with no more than C_1 symmetry. In Table 4, the calculated wavenumbers are compared with the experimental ones. The molecule has an interesting structure with the NH_3 group orientated almost perpendicular to the N−Al−H plane. This obviously implies that the interaction occurs not with the sp^2 orbital of the Al atom, but with its empty p orbital. As a consequence, the $AlNH_2$ unit does not remain planar (the NH_2 group is prevented from π interaction with the Al center). It is worth mentioning that at 212 pm the Al−NH_3 distance is unusually short, about 22 pm shorter than in the Al·NH_3 adduct, and the Al−NH_2 distance is elongated by 13 pm with respect to uncoordinated $HAlNH_2$. The strong coordination of the NH_3 group manifests itself also in an energy of −84.9/−72.3 kJ mol^{-1} (values in the order MP2/DFT) for the formation of $HAlNH_2$·NH_3 from $HAlNH_2$ and NH_3.

Table 4. Comparison between the IR Spectra Observed and Calculated (Wavenumbers in cm^{-1}) for $HAl^{14}NH_2$·$^{14}NH_3$, $HAl^{15}NH_2$·$^{15}NH_3$, and $DAl^{14}ND_2$·$^{14}ND_3$

$HAl^{14}NH_2$·$^{14}NH_3$		$HAl^{15}NH_2$·$^{15}NH_3$		$DAl^{14}ND_2$·$^{14}ND_3$	assign-
obsd	calcd[a]	obsd	calcd[a]	calcd[a]	ment
b	3543.4 (9)	*b*	3534.0 (8)	2608.1 (7)	ν_1
b	3496.8 (31)	*b*	3487.7 (30)	2574.2 (17)	ν_2
b	3473.6 (27)	*b*	3464.6 (26)	2556.5 (15)	ν_3
b	3459.2 (3)	*b*	3454.4 (3)	2502.8 (6)	ν_4
b	3359.9 (5)	*b*	3357.7 (5)	2401.7 (1)	ν_5
1739.3	1750.2 (271)	1738.9	1750.4 (270)	1260.2 (144)	ν_6
b	1610.4 (20)	*b*	1607.8 (20)	1166.3 (9)	ν_7
b	1590.2 (27)	*b*	1587.5 (27)	1152.5 (14)	ν_8
b	1532.8 (26)	*b*	1528.5 (24)	1135.5 (28)	ν_9
1196.2	1191.4 (131)	1178.0/ 1182.5	1185.2 (128)	908.6 (85)	ν_{10}
734.7	755.5 (119)	730.7	752.4 (118)	668.5 (66)	ν_{11}
b	710.5 (86)	*b*	702.7 (92)	580.0 (55)	ν_{12}
b	685.7 (33)	*b*	680.4 (27)	514.4 (29)	ν_{13}
b	615.4 (12)	*b*	611.1 (11)	473.7 (9)	ν_{14}
b	514.1 (26)	*b*	513.9 (26)	372.1 (25)	ν_{15}
b	460.3 (44)	*b*	458.6 (31)	360.9 (49)	ν_{16}
b	447.7 (101)	*b*	446.2 (112)	332.6 (6)	ν_{17}
b	359.8 (5)	*b*	354.1 (5)	316.5 (22)	ν_{18}
b	317.8 (15)	*b*	317.6 (15)	226.7 (9)	ν_{19}
c	224.1 (1)	*c*	224.3 (1)	156.8 (1)	ν_{20}
c	169.3 (6)	*c*	165.9 (6)	151.9 (5)	ν_{21}

[a] Symmetry C_1. Intensities (km mol^{-1}) are given in parentheses. [b] Too weak to be observed or hidden by NH_3 absorptions. [c] Out of the range of detection.

$Al(NH_2)_2$, E. As already mentioned, we had previously made a tentative assignment of some of the IR absorptions of **E** to the adduct $HAlNH_2$·NH_3.[11] Our new experiments, with photolysis conditions different from those used in the

Table 5. Comparison between the IR Spectra Observed and Calculated (Wavenumbers in cm^{-1}) for $Al(^{14}NH_2)_2$, $Al(^{15}NH_2)_2$, and $Al(^{14}ND_2)_2$

$Al(^{14}NH_2)_2$		$Al(^{15}NH_2)_2$		$Al(^{14}ND_2)_2$			
obsd	calcd[a]	obsd	calcd[a]	obsd	calcd[a]	assignment	description of vibrational mode
b	3602.8 (16)	*b*	3592.9 (15)	*b*	2652.5 (16)	$\nu_1(a_1)$	ν(N−H)
b	3508.2 (3)	*b*	3503.1 (3)	*b*	2536.1 (4)	$\nu_2(a_1)$	ν(N−H)
b	1536.7 (8)	*b*	1526.3 (8)	*b*	1139.2 (12)	$\nu_3(a_1)$	$\delta_{sym}(NH_2)$ scissoring
748.2	749.8 (111)	738.2	741.7 (110)	*b*	683.5 (58)	$\nu_4(a_1)$	ν_{sym}(Al−N)
b	673.3 (2)	*b*	660.9 (1)	*b*	549.5 (28)	$\nu_5(a_1)$	δ(N−Al−N)
c	232.7 (3)	*c*	228.9 (3)	*c*	203.8 (2)	$\nu_6(a_1)$	
c	386.3 (0)	*c*	385.9 (0)	*c*	280.2 (0)	$\nu_7(a_2)$	
c	338.7 (0)	*c*	338.1 (0)	*c*	244.9 (0)	$\nu_8(a_2)$	
b	3603.3 (27)	*b*	3593.4 (27)	*b*	2652.5 (14)	$\nu_9(b_1)$	ν(N−H)
3485.3	3504.0 (9)	*b*	3498.9 (8)	*b*	2532.9 (16)	$\nu_{10}(b_1)$	ν(N−H)
1525.1	1506.6 (50)	1520.0	1507.2 (47)	1149.5	1129.8 (66)	$\nu_{11}(b_1)$	$\delta_{asym}(NH_2)$ scissoring
833.4	824.0 (118)	821.4	811.6 (115)	*b*	784.3 (86)	$\nu_{12}(b_1)$	ν_{asym}(Al−N)
b	616.9 (0.3)	*b*	614.4 (0.3)	*b*	459.6 (0.3)	$\nu_{13}(b_1)$	NH_2 wagging
b	459.3 (31)	*b*	459.3 (31)	*b*	326.0 (17)	$\nu_{14}(b_2)$	
b	365.4 (249)	*b*	364.4 (246)	*b*	272.2 (150)	$\nu_{15}(b_2)$	

[a] Symmetry C_{2v}. Intensities (km mol^{-1}) are given in parentheses. [b] Too weak to be observed or hidden by NH_3 absorptions. [c] Out of the range of detection or IR silent.

previous work, show that the signals due to **E** and free $HAlNH_2$ (species **C**) appear (and decay) at different stages of our photolysis. In fact, species **D** can be clearly identified as the adduct $HAlNH_2{\cdot}NH_3$, and our theoretical results lend strong support for such an assignment, as outlined in the previous section. The experiments also leave little doubt that **D** is the precursor to species **E**. Hence, we are encouraged to identify **E** as $Al(NH_2)_2$, which is then formed by elimination of hydrogen from $HAlNH_2{\cdot}NH_3$ (see later).

The normal modes of such a molecule in its energy minimum geometry with C_{2v} symmetry span the irreducible representation ($6a_1 + 2a_2 + 5b_1 + 2b_2$). Our experiments hit on the four most intense IR absorptions of the molecule, the others being either too weak or hidden by NH_3 absorptions. Of these four observed absorptions, the one at 3485.3 cm^{-1} can be assigned to one of the four ν(N−H) stretching fundamentals, which couples only weakly with other fundamentals. The signal at 1525.1 cm^{-1} occurs in a region where the scissoring mode of an NH_2 group is expected to show. Finally, the two modes at 833.4 and 748.2 cm^{-1} involve symmetric and antisymmetric ν(Al−N) stretching motions, but mode coupling occurs. In the absence of any mode coupling, the relative intensities of these two modes would give an estimate for the N−Al−N angle. However, an unrealistic value of 86° is derived from the adaptation of the formula for simple AB_2 compounds or molecules for which the antisymmetric and symmetric stretching fundamentals can be realistically factored out from the vibrational secular equation.[31] It is clear that in this case the two modes include motions of not only the NH_2 units relative to the Al center, but also the H atoms relative to the N atoms, and therefore, the simple formula is not valid. The N−Al−N angle as derived from our calculations is ∼120° and is thus comparable with the H−Al−N angle of $HAlNH_2$ (∼116°).

E, $Al(NH_2)_2$

As expected, our calculations resulted in a global minimum structure with C_{2v} symmetry for $Al(NH_2)_2$. Table 5 includes the calculated wavenumbers and IR intensities associated with all the vibrational fundamentals together with the experimental values. The structure is characterized by Al−N and N−H distances of 178.72 pm and 101.7/101.9 pm. Figure 4 shows the SOMO of $Al(NH_2)_2$. There is a substantial contribution at the Al, but the degree of delocalization is evident.

The force constant f(Al−N) derived from normal coordinate analysis was 364.3 N m^{-1}. Table 6 and Figure 5 compare this value with the corresponding parameters found for $Al{\cdot}NH_3$, AlN, $AlNH_2$, $HAlNH_2$, $Al(NH_2)_2$, and H_2AlNH_2, all of which are experimentally accessible. The force constants can clearly be grouped in three classes: (a) AlN and the monovalent compound $AlNH_2$, (b) the divalent compounds $HAlNH_2$ and $Al(NH_2)_2$, and (c) the trivalent compound H_2AlNH_2.

Barriers to Pyramidalization/Planarization. To evaluate further the bonding in the compounds, we have calculated the barriers to pyramidalization (see **1** for $Al(NH_2)_2$). Using DFT methods, we obtained a value of 48.3 kJ mol^{-1} for $Al(NH_2)_2$, and this can be regarded as a measure of the π stabilization of the molecule.

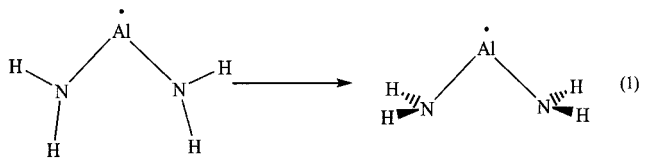

(1)

In Figure 6, this value is compared with the values calculated for NH_3, $HAlNH_2$, and $HAlNH_2{\cdot}NH_3$. Note that

(30) Simons, J. D.; McDonald, J. K. *J. Mol. Spectrosc.* **1972**, *41*, 584.
(31) See, for example: Beattie, I. R.; Ogden, J. S.; Price, D. D. *J. Chem. Soc., Dalton Trans.* **1982**, 505. Himmel, H.-J.; Downs, A. J.; Greene, T. M. *J. Am. Chem. Soc.* **2000**, *122*, 922.

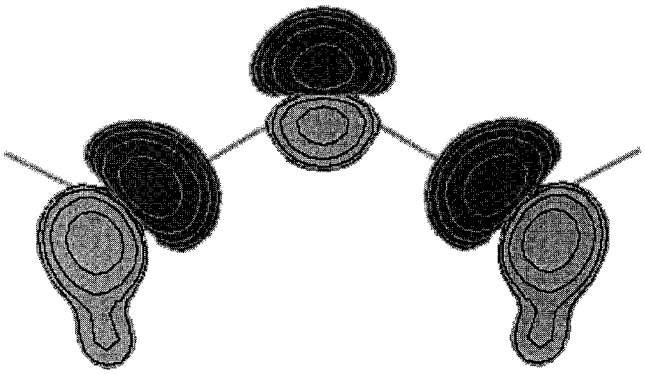

Figure 4. Plot showing the shape of the SOMO of $Al(NH_2)_2$.

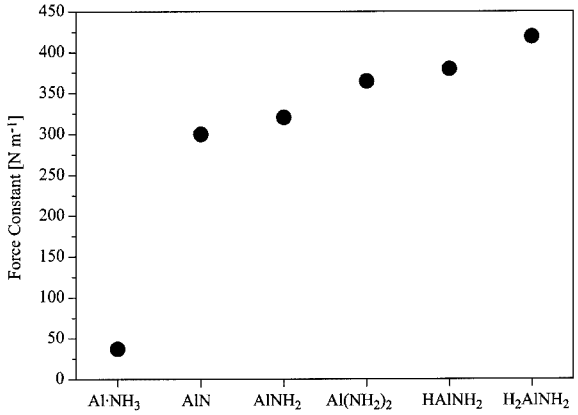

Figure 5. Force constants as derived from normal coordinate analysis for the species $Al{\cdot}NH_3$, AlN, $AlNH_2$, $Al(NH_2)_2$, $HAlNH_2$, and H_2AlNH_2.

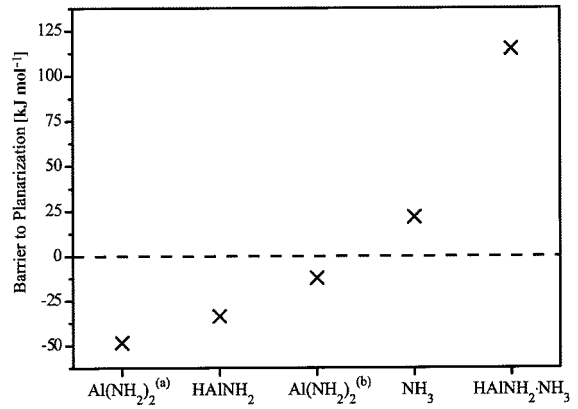

Figure 6. Barriers to planarization at the N atom for the compounds NH_3, $HAlNH_2$, $HAlNH_2{\cdot}NH_3$, and $Al(NH_2)_2$. Note that the barriers are negative for $HAlNH_2$ and $Al(NH_2)_2$, which have a planar energy minimum symmetry. Barriers for $Al(NH_2)_2$ with (a) two and (b) one pyramidalized NH_2 group.

Table 6. Force Constants f(Al−N) (in N m^{-1}) for the Compounds $Al{\cdot}NH_3$, AlN, $AlNH_2$, $HAlNH_2$, $Al(NH_2)_2$, and H_2AlNH_2

compound	f(Al−N)/N m^{-1}	ref
$Al{\cdot}NH_3$	36.9	13, this work
AlN	299.8	30
$AlNH_2$	320.1	13, this work
$Al(NH_2)_2$	364.3	this work
$HAlNH_2$	379.5	13, this work
H_2AlNH_2	419.0	13, this work

the values refer to the barriers to planarization of the pyramidalized molecules. The barriers are positive for NH_3 and $HAlNH_2{\cdot}NH_3$ because both are pyramidal at the nitrogen atom, in their global energy minimum structures, whereas the barriers for $HAlNH_2$ and $Al(NH_2)_2$ are negative because these species are planar in their global energy minimum geometries. As already mentioned, the N atom of the NH_3 group of $HAlNH_2{\cdot}NH_3$ is located almost perpendicular to the plane defined by the H−Al−N fragment for the molecule in its energy minimum form featuring a pyramidal NH_2 unit. However, for the molecule with a planarized $HAlNH_2$ unit, the N atom of the NH_3 group lies within the H−Al−N plane (see **2**). $Al(NH_2)_2$ has the highest negative energy and thus the highest degree of π interaction of the species considered.

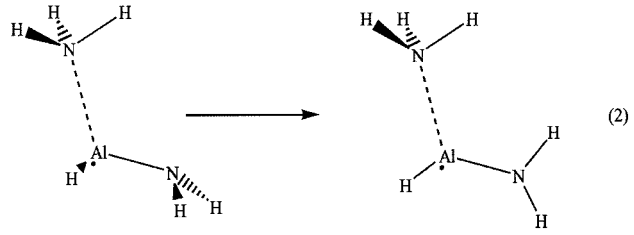

(2)

Reaction Mechanisms. We are now in the position to present detailed schemes for the reactions of one Al atom with one or two NH_3 molecules taking place in solid Ar matrixes (see Scheme 1). The Al atoms react thermally to give the adduct species $Al{\cdot}NH_3$ and $Al(NH_3)_2$, with electron donation in the direction $H_3N \rightarrow Al$. The reaction energy for the formation of $Al{\cdot}NH_3$ amounts to −45.7/−51.1 kJ mol^{-1}. At −79.6/−82.4 kJ mol^{-1}, the energy for the formation of $Al(NH_3)_2$ is less than twice this energy. Insertion leading to $HAlNH_2$ can be achieved either by photolysis into the absorption maximum of $Al{\cdot}NH_3$ or alternatively by supplying IR radiation to overcome the thermal barrier.

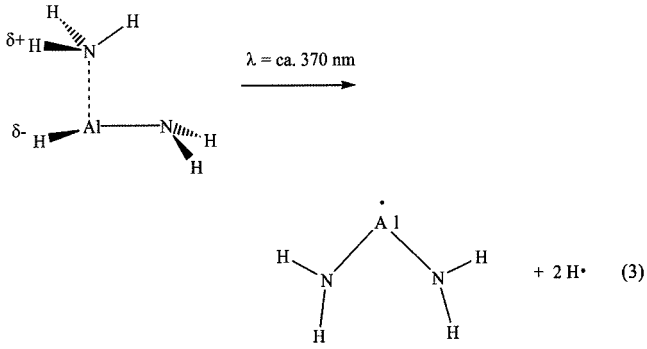

(3)

However, $HAlNH_2$ is not robust to photolysis at $\lambda = 410$ nm but slowly releases hydrogen atoms with the formation of $AlNH_2$ and, in a secondary reaction, H_2AlNH_2. This process has already been discussed in a previous paper.[11] The adduct $HAlNH_2{\cdot}NH_3$ is not accessible by photolysis at $\lambda = \sim 410$ nm because it is immediately destroyed under these conditions, with $Al(NH_2)_2$ being the detectable reaction product. However, it can be formed, like $HAlNH_2$, under the action of IR radiation. The tautomerization of $Al{\cdot}NH_3$ to the insertion product is exothermic by −103.3/−85.3 kJ mol^{-1}. The formation of $HAlNH_2{\cdot}NH_3$ starting from $Al(NH_3)_2$ is exothermic by −154.4/−126.3 kJ mol^{-1}. Photolysis of a matrix containing both $HAlNH_2$ and its adduct $HAlNH_2{\cdot}NH_3$ with light having $\lambda = \sim 370$ nm leads then to

Scheme 1. Reaction Schemes for the Reaction of Al Atoms with (a) One NH_3 Molecule and (b) Two NH_3 Molecules

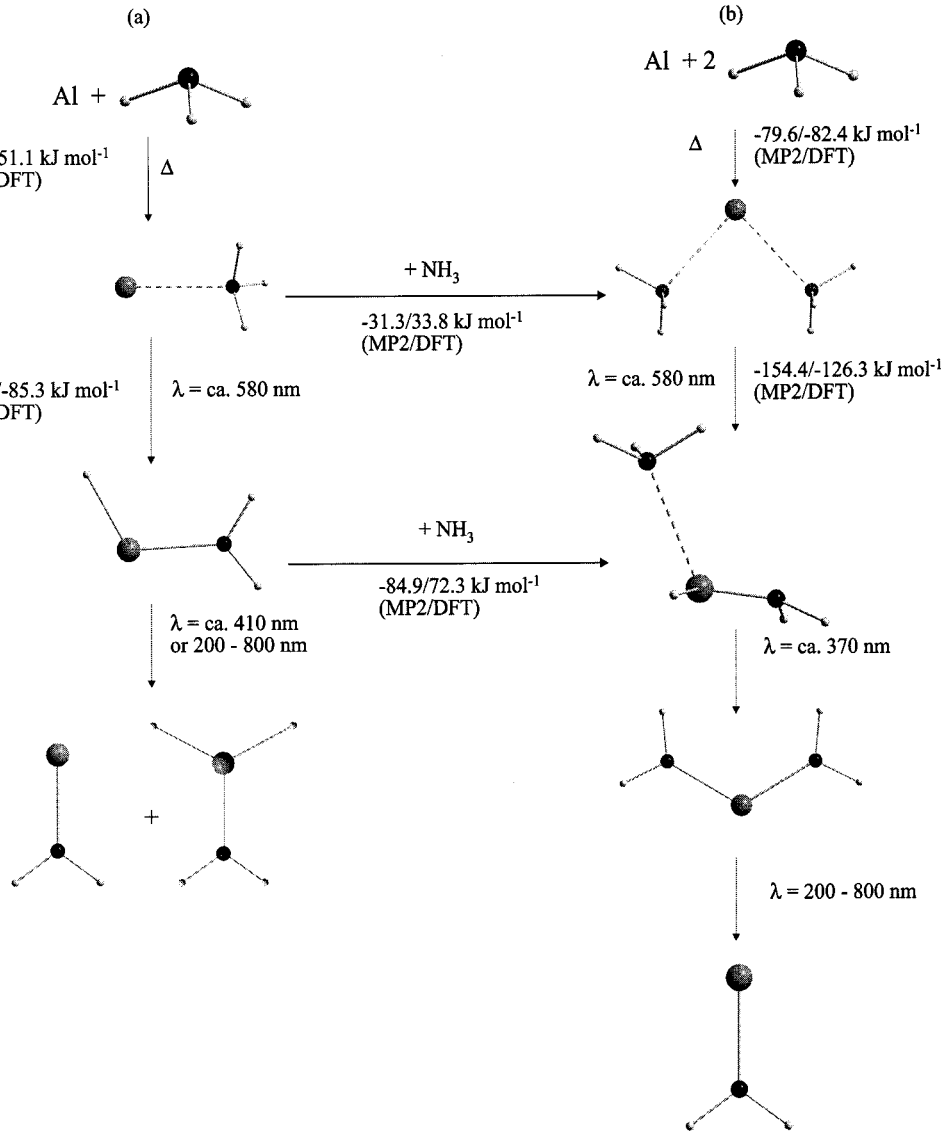

the decomposition of $HAlNH_2{\cdot}NH_3$, to give not $HAlNH_2$, but $Al(NH_2)_2$ (see **3**). $Al(NH_2)_2$ then is stable to photolysis at $\lambda = \sim 410$ nm, while $HAlNH_2$ slowly decomposes. However, broad-band UV−vis light brings about decomposition of $Al(NH_2)_2$, presumably through cleavage of one of the Al−N bonds and formation of $AlNH_2$. The released NH_2 radicals are likely then to react with H atoms generated during the decomposition of $HAlNH_2$ to regenerate NH_3.

Conclusions

The reaction of Al atoms with NH_3 was studied experimentally with IR spectroscopy and theoretically by applying ab initio (MP2) as well as DFT (BP) methods. $Al{\cdot}NH_3$, $Al(NH_3)_2$, $HAlNH_2$, $HAlNH_2{\cdot}NH_3$, and $Al(NH_2)_2$, all exhibiting doublet electronic ground states, are among the products, $HAlNH_2{\cdot}NH_3$ and $Al(NH_2)_2$ being identified and characterized in the experiments described herein for the first time. The matrix isolation technique thus allows the generation and characterization of formally Al(0) and Al(II) compounds, which otherwise elude detection. The pathways leading to all these species were established. Thus, for example, $Al(NH_2)_2$ is formed from $HAlNH_2{\cdot}NH_3$ by photolytically induced elimination of two hydrogen atoms. The sum of all the experimental and theoretical results provides the basis for detailed evaluation of the properties of these species. The results show that the unpaired electron of each species is generally located near the Al center. The experimental and theoretical IR spectra, as well as the electron density distribution in the adducts $Al{\cdot}NH_3$ and $Al(NH_3)_2$, were employed to evaluate the electron donation capacity of the NH_3 group. There are π interactions present to some extent in the other molecules which lead to some delocalization of the unpaired electron. The barriers for pyramidalization at the nitrogen atoms were used to probe the amount of this π interaction. The largest barrier was found for $Al(NH_2)_2$. In contrast to the free $HAlNH_2$ molecule, which exhibits a planar energy minimum structure, the adduct with ammonia, $HAlNH_2{\cdot}NH_3$, which was clearly identified by its IR spectrum, is pyramidal at the N atom. The angle of about 90° between the N atom of the NH_3 group and the H−Al−N

plane indicates that the interaction between $HAlNH_2$ and NH_3 mainly occurs through the Al p orbital which is then not free to stabilize a planar $HAlNH_2$ unit. For all the molecules, the f(Al−N) force constants (derived from normal coordinate analysis) show a clear trend in the direction Al(I) < Al(II) < Al(III).

Acknowledgment. The authors thank (a) the Deutsche Forschungsgemeinschaft for financial support and the award of a Habilitationsstipendium to H.-J.H., and (b) Dr. Kasai for fruitful discussions.

IC011292N